Colon Flattening by Landmark-Driven Optimal Quasiconformal Mapping

Wei Zeng[1] and Yi-Jun Yang[1]

[1] Florida International University, Miami, Florida 33199, USA
[2] Shandong University, Jinan, Shandong 250101, China

Abstract. In virtual colonoscopy, colon conformal flattening plays an important role, which unfolds the colon wall surface to a rectangle planar image and preserves local shapes by conformal mapping, so that the cancerous polyps and other abnormalities can be easily and thoroughly recognized and visualized without missing hidden areas. In such maps, the anatomical landmarks (taeniae coli, flexures, and haustral folds) are naturally mapped to convoluted curves on 2D domain, which poses difficulty for comparing shapes from geometric feature details. Understanding the nature of landmark curves to the whole surface structure is meaningful but it remains challenging and open. In this work, we present a novel and effective colon flattening method based on quasiconformal mapping, which straightens the main anatomical landmark curves with least conformality (angle) distortion. It provides a canonical and straightforward view of the long, convoluted and folded tubular colon surface. The computation is based on the holomorphic 1-form method with landmark straightening constraints and quasiconformal optimization, and has linear time complexity due to the linearity of 1-forms in each iteration. Experiments on various colon data demonstrate the efficiency and efficacy of our algorithm and its practicability for polyp detection and findings visualization; furthermore, the result reveals the geometric characteristics of anatomical landmarks on colon surfaces.

1 Introduction

Colorectal cancer is the third most commonly diagnosed cancer in the world. Conventional optical colonoscopy (OC) [1] was invented for screening precancerous polyps, but it requires invasive operation and causes harms and pains to patients. Virtual colonoscopy (VC), also called computerized tomography (CT) colonography [2,3] provides a more comfortable and non-invasive alternative diagnosis; it requires to extract 3D colon inner wall surface from CT scans of the abdomen first, and then the radiologist can "fly" through the virtual 3D colon tunnel to locate the precancerous polyps and cancer. The colon is a long and convoluted tube structure, so the VC method is time-consuming and has difficulty to have a complete check if the colon is occluded.

Colon flattening was introduced to generate a global and complete visualization of the entire colon wall, where the convoluted and folded surface are

P. Golland et al. (Eds.): MICCAI 2014, Part II, LNCS 8674, pp. 244–251, 2014.

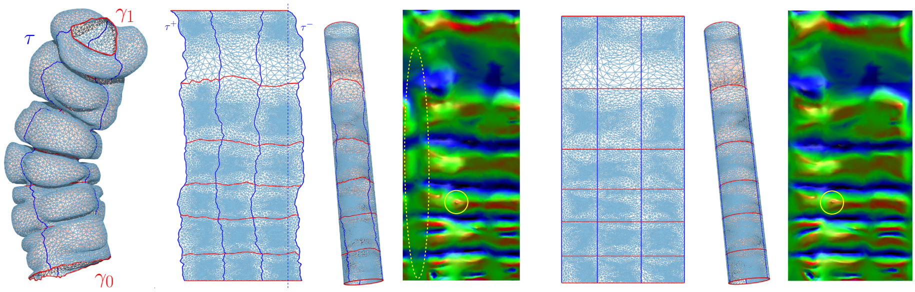

(a) colon - I (b) conformal map (c) optimal quasiconformal map

Fig. 1. Colon flattening by landmark-driven quasiconformal mapping. (a) shows a colon segment with 5 haustral folds (red) and 3 taeniae coli (blue) landmarks (5h, 3v). Frames in (b-c) respectively denote planar map, cylinder map, and flattened image color-encoded by mean curvatures of the 3D colon surface. The yellow dashed ellipse illustrates the area with broken taeniae coli on rectangle conformal view.

flattened onto a planar domain; by this mapping, geometric and intensity information of the original 3D surface can be fully exposed on the 2D domain. Therefore, polyps and abnormalities can be efficiently obtained with computer aided detection (CAD) techniques on the 2D flattened view and easily located on 3D endoluminal view by the mapping [4]. A plausible method is conformal mapping (C-map), which preserves angles (local shapes) and therefore is highly desired for morphometry based medical diagnosis. Colon conformal flattening has been well studied in recent works; the methods include Laplace-Beltrami operator [5], holomorphic 1-form [6] and curvature flow [7]. In addition, a curved 2D flattening view based on harmonic map [8] was presented.

In medical imaging, biomarkers or anatomical landmarks are commonly used to assist shape analysis and abnormality diagnosis. Significant anatomical landmarks of colon surfaces are taeniae coli (three bands of longitudinal muscles which run from the caecum to the rectum, located between latitudinal haustral folds) and flexures (sharp bends of the colon, connecting two components) haustral folds are also helpful. These landmarks appear as irregular or broken curves on 2D rectangle conformal views (Fig. 1(b)), which decreases the efficiency of polyp or tumor screening. In this work, we present a novel colon flattening method using the insight from quasiconformal geometry [9]. The flattening is formulated as a quasiconformal mapping (QC-map), where the taeniae coli and flexures (or haustral folds) are mapped to vertical and horizontal straight lines on the rectangle (Fig. 1(c)) and the conformality distortion introduced is minimized (Fig. 2). These landmarks characterize primary anatomical geometry of colon surface. With them, straightened QC map provides a well-structured view, representing both local and global geometric structures, which is more accessible for reading or automatic screening than conformal views with broken features.

The desired quasiconformal mapping is obtained by adapting the holomorphic 1-form with landmark straightening constraints to be a unique and optimal quasi-holormophic 1-form. Holomorphic 1-forms have been well studied and applied to computer graphics, vision and medical imaging fields [10], [4], [11] The desired quasi-holomorphic 1-form is formulated as a pair of conjugate differential 1-forms (each is a harmonic 1-form plus an exact 1-form) based on Hodge decomposition theorem [12], and can be computed through harmonic energy minimization with the given landmark straightening constraints. The integration of this 1-form gives a quasiconformal mapping associated with a Beltrami coefficient μ. Followed by an iterative harmonic quasiconformal optimization process, the value of $\max|\mu|$ is minimized. The final optimal map gives the intrinsic and unique structure of the surface paired with its landmarks. This technique is called quasiconformal straightening (QCS), which is useful for feature-aware visualization, matching, registration, and shape analysis.

Based on this algorithm, one can have a straightforward canonical view for the long, convoluted and folded tubular colon surface. We use the pullback metric to describe the variation of conformal structures of *decorated surface* (S, L) (L is a set of landmark curves) from *pure surface* S, using the conformal module of the 2D rectangle domain, $Mod = h/w$, the ratio of height h and width w, which is a conformal invariant. In Fig. 1, $Mod(S) = 2.32$, $Mod(S, L) = 2.18$. The new canonical shape representation reveals the characteristics of the anatomical landmark curves with respect to the whole surface geometry. Experiment results on a set of colon surfaces under different modalities demonstrate the efficiency and efficacy of our algorithm for colon flattening and further finding verification.

To our best knowledge, this is the *first* work to flatten colon surfaces associated with straightening anatomical landmarks (taenie coli, flexures, or haustral folds) with the least conformality (angle) distortion. The proposed QCS technique based on 1-form method has linear time complexity and is robust to topology and geometry noises. It can handle multiple and complicated landmark curves, and is general for surfaces with more complicated topologies.

2 Theoretic Background

This section briefly introduces the background knowledge of conformal geometry and quasiconformal geometry. For more details, we refer readers to [13,12,9].

2.1 Holomorphic 1-Forms

A *holomorphic 1-form* on a Riemann surface S is an assignment of a holomorphic function $\phi_i(z_i)$ on each chart z_i such that if z_j is another local coordinate, then $\phi_i(z_i) = \phi_j(z_j)(\frac{dz_j}{dz_i})$. It has the representation $\omega = \tau + i^*\tau$, where τ is a *harmonic 1-form*, $\tau = df$, $\Delta f = 0$. The Laplacian-Beltrami operator $\Delta = d\delta + \delta d$, where d is the exterior derivative, δ is the codifferential. In each cohomology class, there exists a unique harmonic 1-form. Hodge decomposition theorem [12] says that any 1-form ω can be decomposed to three forms, an exact form $d\alpha$, a closed form

$\delta\beta$ and a harmonic form γ, where α is a 0-form. Adapting the unique harmonic 1-form by an exact 1-form results in a new differential 1-form.

2.2 Conformal Mapping and Quasiconformal Mapping

Suppose $f : (S_1, \mathbf{g}_1) \to (S_2, \mathbf{g}_2)$ is a differential mapping between two Riemann surfaces, S_1, S_2 with Riemannian metric $\mathbf{g}_1, \mathbf{g}_2$ respectively. It is called a *conformal mapping* if its local representation $w(z)$ satisfies $\partial_{\bar{z}} w = 0$ everywhere. The complex differential operators are defined as $\partial_z = \frac{1}{2}(\partial_x - i\partial_y)$ and $\partial_{\bar{z}} = \frac{1}{2}(\partial_x + i\partial_y)$. In general, the mapping f satisfies the *Beltrami equation*,

$$\partial_{\bar{z}} f = \mu_f(z) \partial_z f, \tag{1}$$

where μ is called the *Beltrami coefficient*, $\|\mu\|_\infty < 1$. If $\mu = 0$, then f is a holomorphic function, which preserves angles and is conformal. If $\|\mu_f\|_\infty < k$, then f is a *quasiconformal mapping* with bounded angle distortion, which is uniquely determined by its μ, and vice versa.

3 Algorithm

The main goal of our algorithm is to compute the unique and optimal quasiconformal mapping with landmark straightening constraints for the tubular colon surface. The computational pipeline is as follows:

Step 1: Slice Surface Open. We puncture a small hole at each end such that the colon becomes a topological cylinder with two boundaries. The surface is represented by a triangular mesh, denoted as $M = (V, E, F)$, where V, E, F are vertex, edge and face sets respectively; the boundary is $\partial M = \gamma_0 - \gamma_1$, where γ_0, γ_1 denote the exterior and interior boundaries respectively; a set of landmark curves on M is denoted as $L = L^H \cup L^V$, where landmarks in L^H are mapped to horizontal segments, landmarks in L^V to vertical segments.

We the slice the colon surface open by the shortest path τ connecting two boundaries. The the colon surface becomes a topological quadrilateral M', where τ is split into two opposite boundary segments τ^+, τ^-, as shown in Fig. 1(a).

Step 2: Compute Quasi-holomorphic 1-forms. Assume the mapping is $f : (M, L) \to (D, \ell)$, D has local coordinates (u, v). The algorithm is as follows:

1. Compute two constrained harmonic function f_1, f_2,

$$\begin{cases} \Delta f_1 = 0 \\ f_1|_{\tau^+} = 0 \\ f_1|_{\tau^-} = 1 \\ \frac{\partial f_1}{\partial \mathbf{n}}|_{\gamma_0 \bigcup \gamma_1} = 0 \\ f_1|_{l_j} = t_j, l_j \in L^V \end{cases} \quad \text{and} \quad \begin{cases} \Delta f_2 = 0 \\ f_2|_{\gamma_0} = 0 \\ f_2|_{\gamma_1} = 1 \\ f_2|_{l_i} = s_i, l_i \in L^H \end{cases},$$

   where $\mathbf{n}$ is the normal vector to the boundary, s_i, t_j are unknown variables, computed automatically. Landmark curve, $l_k = [v_1, v_2, \ldots, v_{n_k}]$, has two types of straightening constraints, as follows:

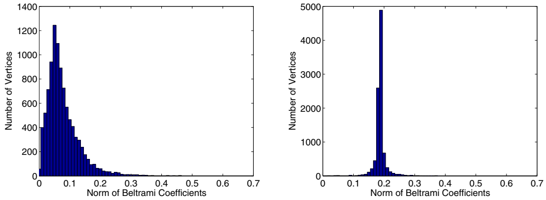

(a) initial $|\mu_0|$ (b) optimal $|\mu_n|$

Fig. 2. Histograms of conformality distortion in quasiconformal optimization

- *Horizontal*: v coordinates are same, $v(v_1) = v(v_2) = \ldots = v(v_{n_i}) = s_i$.
- *Vertical*: u coordinates are same, $u(v_1) = u(v_2) = \ldots = u(v_{n_j}) = t_j$.

The Laplace-Beltrami operator Δ is approximated by cotangent edge weight, $\Delta f(v_i) = \sum_{e[v_i,v_j]\in E} w_{ij}(f(v_i) - f(v_j))$, where $w_{ij} = \frac{1}{2}(\cot\theta_{ij}^k + \cot\theta_{ji}^l)$, $e \notin \partial M$; $w_{ij} = \frac{1}{2}\cot\theta_{ij}^k$, $e \in \partial M$; $\theta_{ij}^k, \theta_{ji}^l$ are the angles against edge $[v_i, v_j]$.

2. Compute harmonic 1-forms by gradient computation, $\tau_1 = \nabla f_1, \tau_2 = \nabla f_2$.
3. Compute conjugate 1-form of τ_1 by Hodge star operator, ${}^\star\tau_1 = \lambda\tau_2$ (λ is a scalar), by minimizing the energy $E(\lambda) = \sum_{[v_i,v_j,v_k]\in F} |\nabla f_2 - \lambda\mathbf{n}\times\nabla f_1|^2 A_{ijk}$, where A_{ijk} is the area of face $[v_i, v_j, v_k]$, $\mathbf{n}$ is the normal vector to the face.
4. Compute $\omega = \tau_1 + \sqrt{-1}\,{}^\star\tau_1$.

Step 3: Compute Quasiconformal Mapping. We generate the quasiconformal mapping by integrating the obtained quasi-holomorphic 1-form ω over the open domain M', $f(p) = \int_{\gamma(q,p)\in M'} \omega$, $\forall p \in V$, where $\gamma(q,p)$ is an arbitrary path from the base vertex q to the current vertex p. On the planar domain, $f(q) = (0,0)$, $f(\gamma_i), f(l_k)$ are all straight lines. We can get the rectangle map by tracing a straight line perpendicular to boundaries $f(\gamma_i)$. We set $f_0 = f$.
Step 4: Optimize Quasiconformal Mapping. The process is as follows:

1. Compute the initial Beltrami coefficient $\mu_0 = \mu(f_0)$ using Eqn. (1).
2. Repeat *1) Optimization*: Diffuse $\mu_{n+1} \leftarrow \mu_n + \delta\Delta\mu_n$. *2) Projection*: a) Compute the intermediate quasiconformal map associated with μ_n, $f^{\mu_n} : (D, z) \to (D^{\mu_n}, \zeta)$; b) Compute the quasiconformal map $h^{\mu_n} : (D^{\mu_n}, L) \to (D, \ell)$ by Steps 2-3; c) Update $\mu_{n+1} \leftarrow \mu(h^{\mu_n} \circ f^{\mu_n})$, Until $\|\mu_{n+1} - \mu_n\|_\infty < \epsilon$.
3. The desired mapping $f = h^{\mu_n} \circ f^{\mu_n} \circ f_0$.

The solution of the quasiconformal optimization process converges to the extremal QC map; the resulted map is unique and optimal (with least conformality distortion $|\mu|$), which is proved by the method in [14]. The initial distribution of $|\mu|$ obtained in Step 3 is scattered (Fig. 2(a)), where large distortions are near landmark curves. The harmonic energy sequence of the maps $\{E(h^{\mu_n})\}$ and max $|\mu|$ in Step 4 monotonically decreases and converges; thus the final $|\mu|$ is the least and becomes uniform [14] (Fig. 2(b) with $\epsilon = 1e-5$). The resulted map avoids local significantly distorted areas which may contain polyps. The 1-form algorithm solves sparse linear systems and has linear time complexity in each iteration. More computational details can be found in [10], [6], [15].

Table 1. Statistics on colon flattening experiments

Model	#vertex	#face	#landmark	time	C-Mod	QC-Mod	max $\|\mu_0\|$	optimal $\|\mu_n\|$
I	9,608	19,105	5h, 3v	10s	2.32	2.18	0.49	0.17
II	19,085	38,114	25h, 3v	40s	9.69	11.04	0.42	0.17
III	16,459	32,827	36h, 3v	35s	8.37	9.17	0.44	0.16

4 Experiments

Colon Data Preprocessing. The proposed algorithms are validated on real VC colon data from the public databases of NIBIB and NIH. In the data preprocessing, we perform digital cleansing, segmentation, denoising [4], and colon inner wall surface extraction [16] on raw CT scans, and then do smoothing, remeshing and simplification on triangular meshes (Fig. 1).

Anatomical Landmark Extraction. We extract the taenia coli and haustral folds on the mean curvature color-encoded conformal mapping images (see Fig. 1(b)). We first extract the skeleton of the blue bands (corresponding to haustral folds), and project them onto 3D surface. By connecting the three disjointing haustral folds at the same latitudinal level we obtain a loop by the shortest path between them. We then perturb each loop to be the locally shortest. In collapsed or bending areas due to occlusions, some haustral folds are missing or cannot be connected. Our algorithm is stable to accept both closed and open landmark curves. We extract taeniae coli by connecting the middle points between two latitudinally consecutive endpoints of haustral folds.

Landmark-Driven Colon Flattening. We tested our algorithms on 45 colon surfaces, including 30 colon segments with 3 taeniae coli (TC) and 15 whole colons where only 1$\sim$2 TC can be automatically extracted (mainly restricted by flat geometry of sigmoid and rectum). The algorithms are tested on a desktop with 3.7GHz CPU and 16GB RAM. The whole pipeline is automatic and is effective, stable and robust for all the tests, due to the linearity of 1-form.

Figures 1 and 3 visually illustrate the C and QC mapping results of 3 examples. We use the yellow ellipses to highlight the areas with broken taenia coli on rectangle conformal flattening images. These areas are straightened on quasiconformal flattening images and the taeniae coli are connected; at the same time, there is no significant shape distortion from conformal flattening. This gives the VC user a global and straightforward view for screening polyps or abnormalities (see Fig. 1, the polyp is labeled in the yellow circle on both C and QC views).

Table 1 gives the corresponding computational statistics, including running time, the initial max $|\mu_0|$ in Step 3 and the optimal $|\mu_n|$ in Step 4. The average max $|\mu_0|$ and optimal $|\mu_n|$ over 45 tests are 0.46 and 0.17, respectively. The max $|\mu|$ is minimized and the distribution of $|\mu_n|$ becomes almost uniform (Fig. 2).

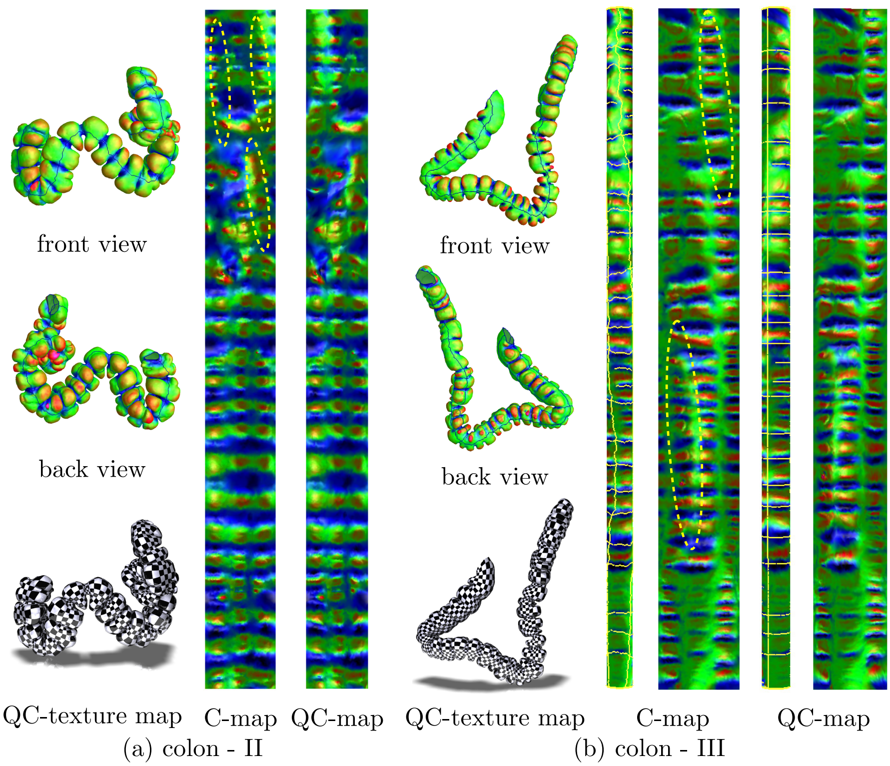

Fig. 3. More examples of landmark-driven quasiconformal colon flattening

Performance Discussion. 1) *Efficiency, Robustness, and Generality*: The 1-form method solves positive definite sparse linear systems, therefore has linear time complexity and is robust to topological and geometric noises. The algorithm is easy to implement, efficient to compute, and robust and stable to handle multiple and complicated decorative landmark curves. The proposed landmark-driven quasiconformal straightening technique can be incorporated into the holomorphic 1-form computation for general topological surfaces [10]. 2) *Novelty, Comparison, and Practicability*: To our best knowledge, this is the first work to flatten colon surfaces while straightening taeniae coli and flexures with least angle distortion guarantee through a canonical quasiconformal mapping. In contrast to existing conformal colon flattening works such as [5], [6], [8], our method uniformizes both surface and decorative landmark geometries. For straightening purpose, registration methods may work but require a manually prescribed target domain; our method automatically generates a unique and intrinsic parameter domain. The proposed straightened map has great potential for feature-aware shape analysis and precise curve-constrained surface registration, such as supine-prone colon registration, 3D colon straightening, and other medical tasks where landmark curves are naturally associated.

5 Conclusion

We present a novel and rigorous colon flattening method, which straightens anatomical landmark curves (taeniae coli, flexures and haustral folds) with least angle distortion. The algorithm generates the unique optimal quasiconformal map for surface decorated with landmark curves based on holomorphic 1-form with landmark constraints and quasiconformal optimization process. The technique discoveries the characteristics of landmark curves and the influence to conformal structure and reveals the canonical structures of convoluted colons. The experimental results on various colon data demonstrate the efficiency and efficacy of our algorithm. The performance shows great potential for colon polyp and abnormality screening. The proposed method is stable and general, and will have broad impacts on shape analysis of any tubular anatomical structures.

References

1. Center, M.M., Jemal, A., Smith, R.A., Ward, E.: Worldwide variations in colorectal cancer. CA: A Cancer Journal for Clinicians 59(6), 366–378 (2009)
2. Vining, D., Shifrin, R., Grishaw, E., Liu, K., Choplin, R.: Virtual colonscopy (abstract). Radiology 193(P), 446 (1994)
3. Hong, L., Muraki, S., Kaufman, A., Bartz, D., He, T.: Virtual voyage: Interactive navigation in the human colon. In: Proc. of SIGGRAPH, pp. 27–34 (1997)
4. Hong, W., Qiu, F., Kaufman, A.: A pipeline for computer aided polyp detection. IEEE TVCG 12(5), 861–868 (2006)
5. Haker, S., Angenent, S., Kikinis, R.: Nondistorting flattening maps and the 3d visualization of colon ct images. IEEE TMI 19, 665–670 (2000)
6. Hong, W., Gu, X., Qiu, F., Jin, M., Kaufman, A.: Conformal virtual colon flattening. In: Proc. of ACM Symposium on Solid and Physical Modeling, pp. 85–93 (2006)
7. Qiu, F., Fan, Z., Yin, X., Kaufman, A., Gu, X.: Colon flattening with discrete Ricci flow. In: Metaxas, D., Axel, L., Fichtinger, G., Székely, G. (eds.) MICCAI 2008 Workshop. LNCS, vol. 5242, pp. 97–102. Springer, Heidelberg (2008)
8. Marino, J., Zeng, W., Gu, X., Kaufman, A.: Context preserving maps of tubular structures. IEEE TVCG 17(2), 1997–2004 (2011)
9. Ahlfors, L.: Lectures in Quasiconformal Mappings. Van Nostrand Reinhold, New York (1966)
10. Gu, X., Yau, S.T.: Global conformal parameterization. In: Proc. of Symposium on Geometry Processing, pp. 127–137 (2003)
11. Zeng, W., Marino, J., Gurijala, K., Gu, X., Kaufman, A.: Supine and prone colon registration using quasi-conformal mapping. IEEE TVCG 16(6), 1348–1357 (2010)
12. Farkas, H.M., Kra, I.: Riemann Surfaces. Springer, New York (1980)
13. Guggenheimer, H.W.: Differential Geometry. Dover Publications (1977)
14. Lui, L.M., Gu, X., Yau, S.T.: Convergence of an iterative algorithm for teichmüller maps via harmonic energy optimization. Technical report (2013), `ftp://ftp.math.ucla.edu/pub/camreport/cam13-36.pdf`
15. Zeng, W., Luo, F., Yau, S.-T., Gu, X.D.: Surface quasi-conformal mapping by solving Beltrami equations. In: Hancock, E.R., Martin, R.R., Sabin, M.A. (eds.) Mathematics of Surfaces XIII. LNCS, vol. 5654, pp. 391–408. Springer, Heidelberg (2009)
16. Gibson, S.F.F.: Constrained elastic surface nets: Generating smooth surfaces from binary segmented data. In: Wells, W.M., Colchester, A.C.F., Delp, S. (eds.) MICCAI 1998. LNCS, vol. 1496, pp. 888–898. Springer, Heidelberg (1998)